MOnItoRing of large scale complex technologicAl systems
(European **MOIRA** project)

Effective Identification of Cyclic Excitation and Resonance in Non-stationary Gearbox Vibration Monitoring

- Mojtaba Ahani

Horizon 2020
European Union Funding
for Research & Innovation

LaMCoS
UMR CNRS5259 / INSA-LYON

Subject of the thesis:

Improving virtual sensing by multicomplexity models

Context:

Monitoring of heterogeneous fleet of machines, using a generic model, and solving an inverse identification problem

Supervisors: *Didier REMOND, Adeline BOURDON*

Host Institution:

Laboratoire de Mécanique des Contacts et des Structures (LaMCoS), INSA Lyon, France

This thesis has been defined as a part of Marie Sklodowska Curie *program through the* **ETN MOIRA** *project (GA 955681) and supported by the European Commission.*

Horizon 2020
European Union Funding
for Research & Innovation

Introduction:

- Physical Versus Virtual Sensors
- Heterogeneous Fleet of Machines

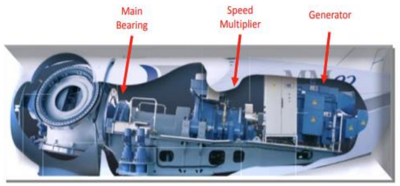

Effective Identification of Cyclic and Resonance Excitations:

- Introduction to the identification approaches
- Description of the Problem and the system modeling
- Identification results

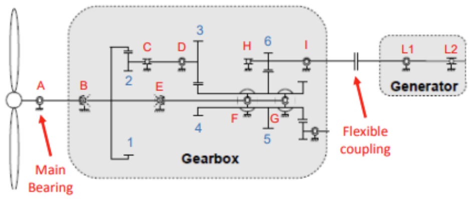

Physical Versus Virtual Sensors:

Drawbacks:

- Limited spatial and temporal coverage
- Uncertainty
- Limited robustness
- Accuracy lost over time

Advantages:

- Significantly lower costs
- Where physical sensors can not be deployed
- Reducing signal noise
- Can recognize and compensate drift phenomenon in physical sensors
- Flexible and can be redesigned as required
- To share the same signal along the fleet of machines

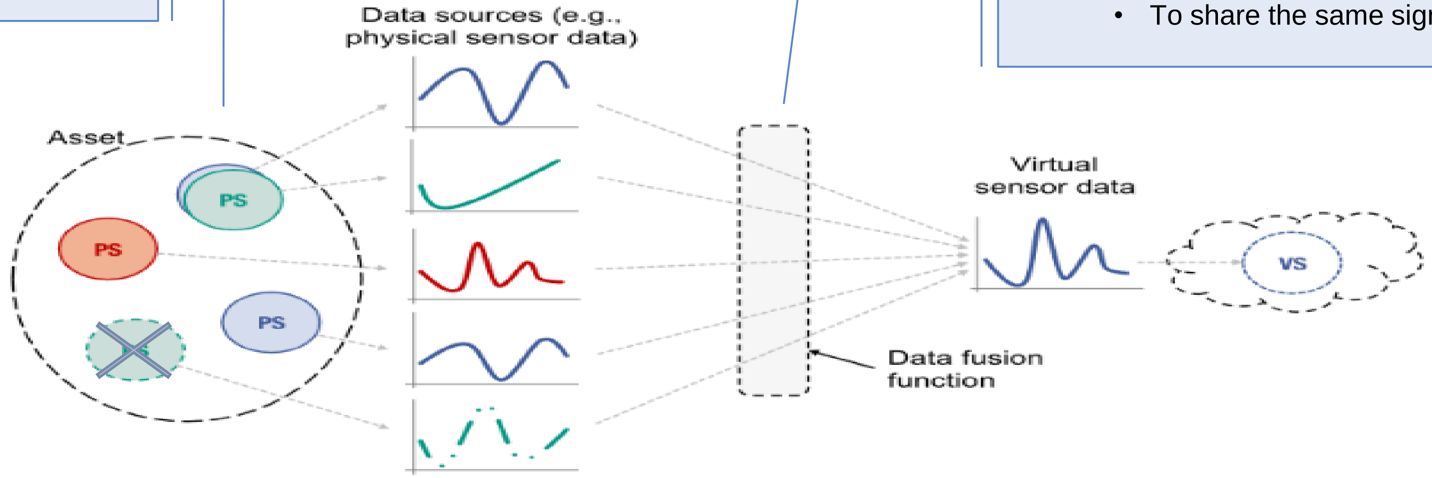

Virtual Sensor Concept,
Martin D, Kühl N, Satzger G. *Virtual sensors*. Business & Information Systems Engineering. 2021 Jun;63:315-23.

Heterogeneous Fleet of Machines

Different Architecture Types

3-Stage Gear Box

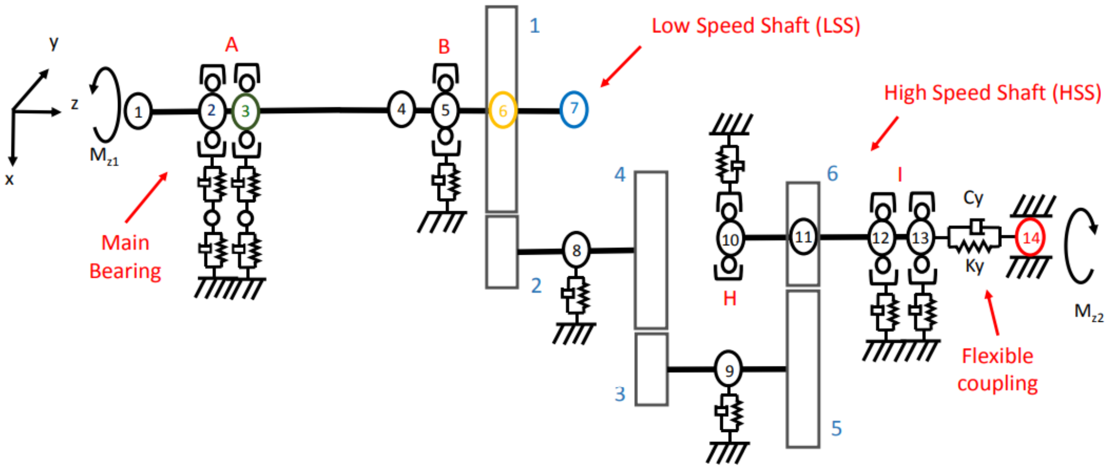

2-Stage Gear Box

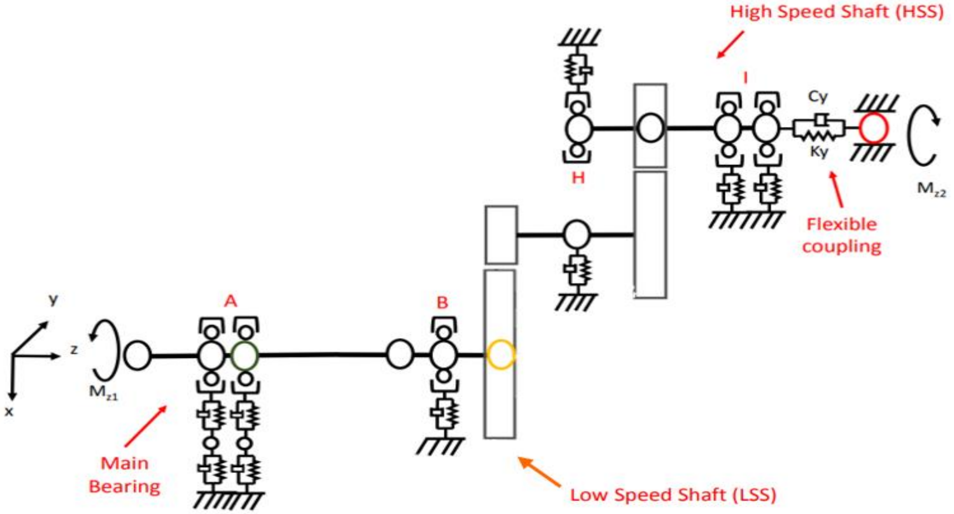

Bearings	Characteristics
A	*Double row spherical. Self-aligning*
B	*Single row tapered*
C	*Double row cylindrical*

Bearings	Characteristics
D	***Double row tapered. Self-aligning***
E	***Single row tapered***
F/G	***Single row cylindrical***

Bearings	Characteristics
H	***Single row tapered***
I	***Double row tapered***
L1 /L2	***Deep groove ball bearings***

Graph Theory:

Layer 1 - Geometry

3-Stage Gear Box

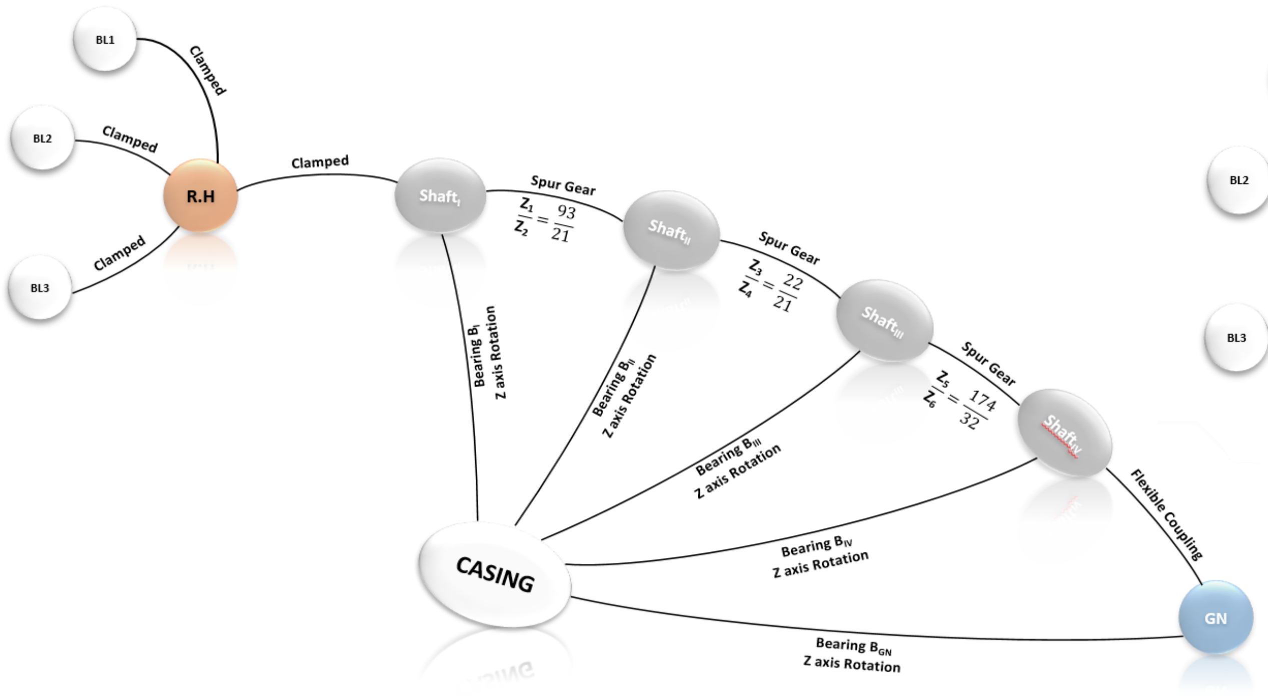

2-Stage Gear Box

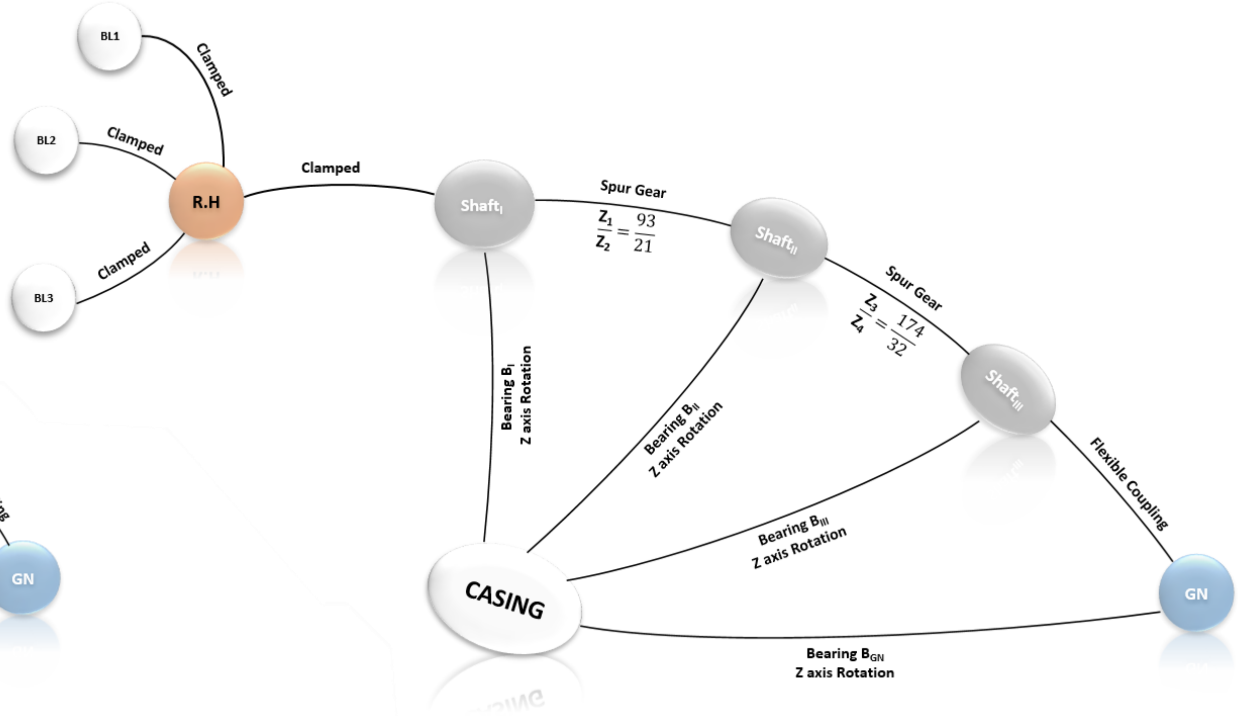

Graph Theory: 2-Stage Gear Box

Layer 1 - Geometry

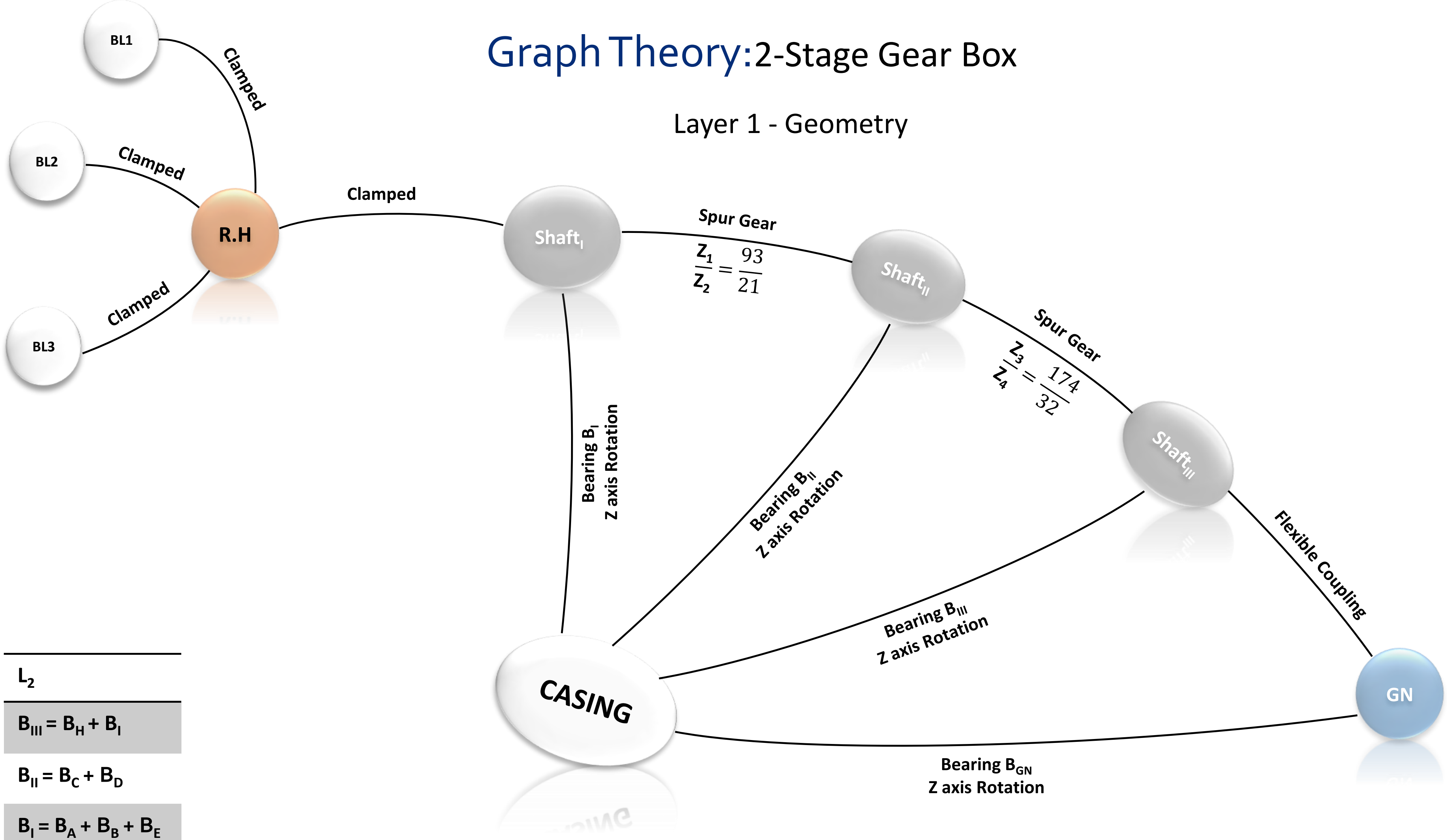

L_2
$B_{III} = B_H + B_I$
$B_{II} = B_C + B_D$
$B_I = B_A + B_B + B_E$

R.H: Rotating Hub
Bl: Blade
Sh: Shaft
GN: Generator

Gear	*Z: Teeth Number*
1	*93*
2	*21*
3	*174*
4	*32*

Graph Theory: 2-Stage Gear Box

Layer 2 – Interaction and Boundary conditions

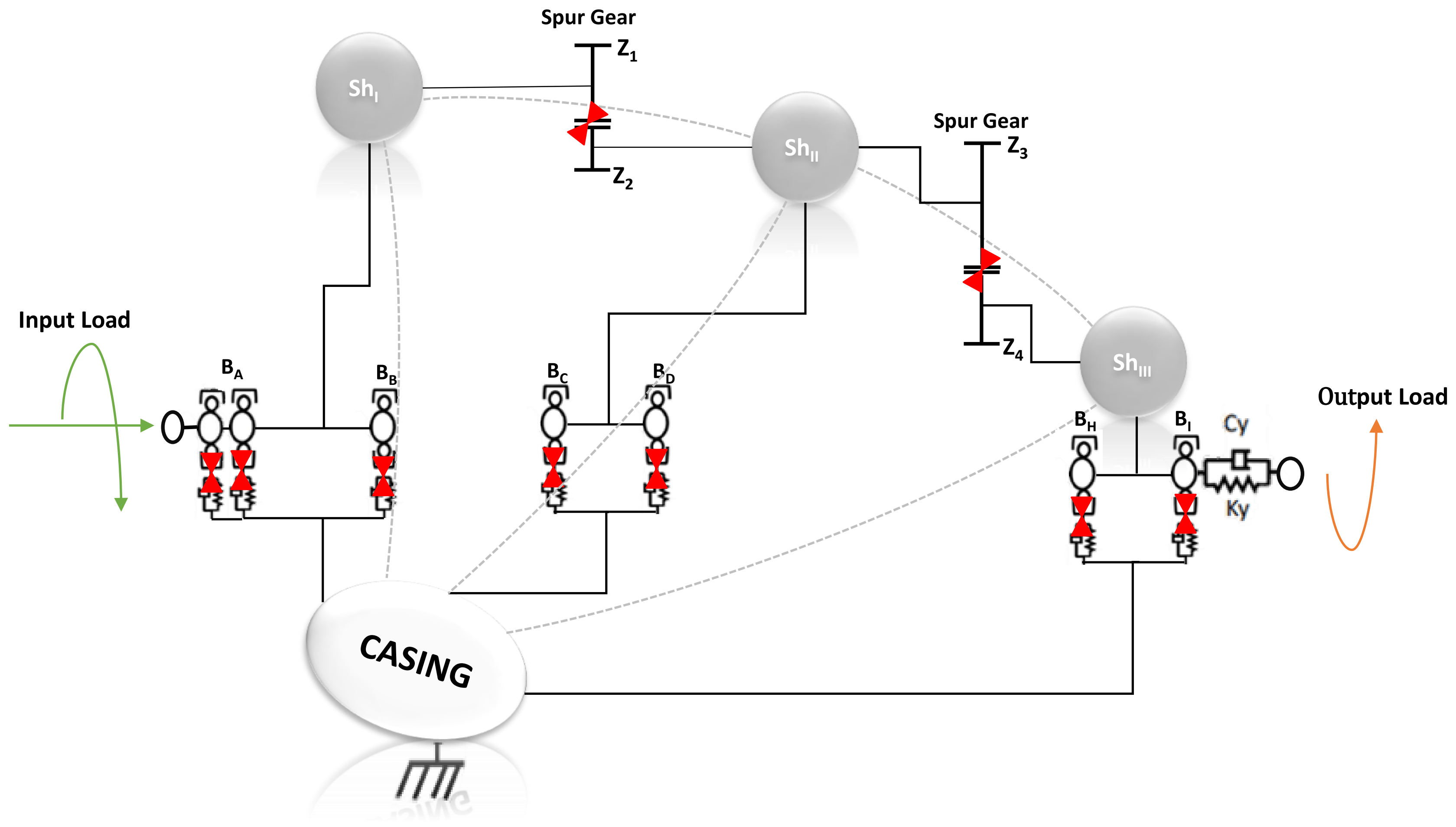

Graph Theory:2-Stage Gear Box

Layer 3 – Physical Sensors

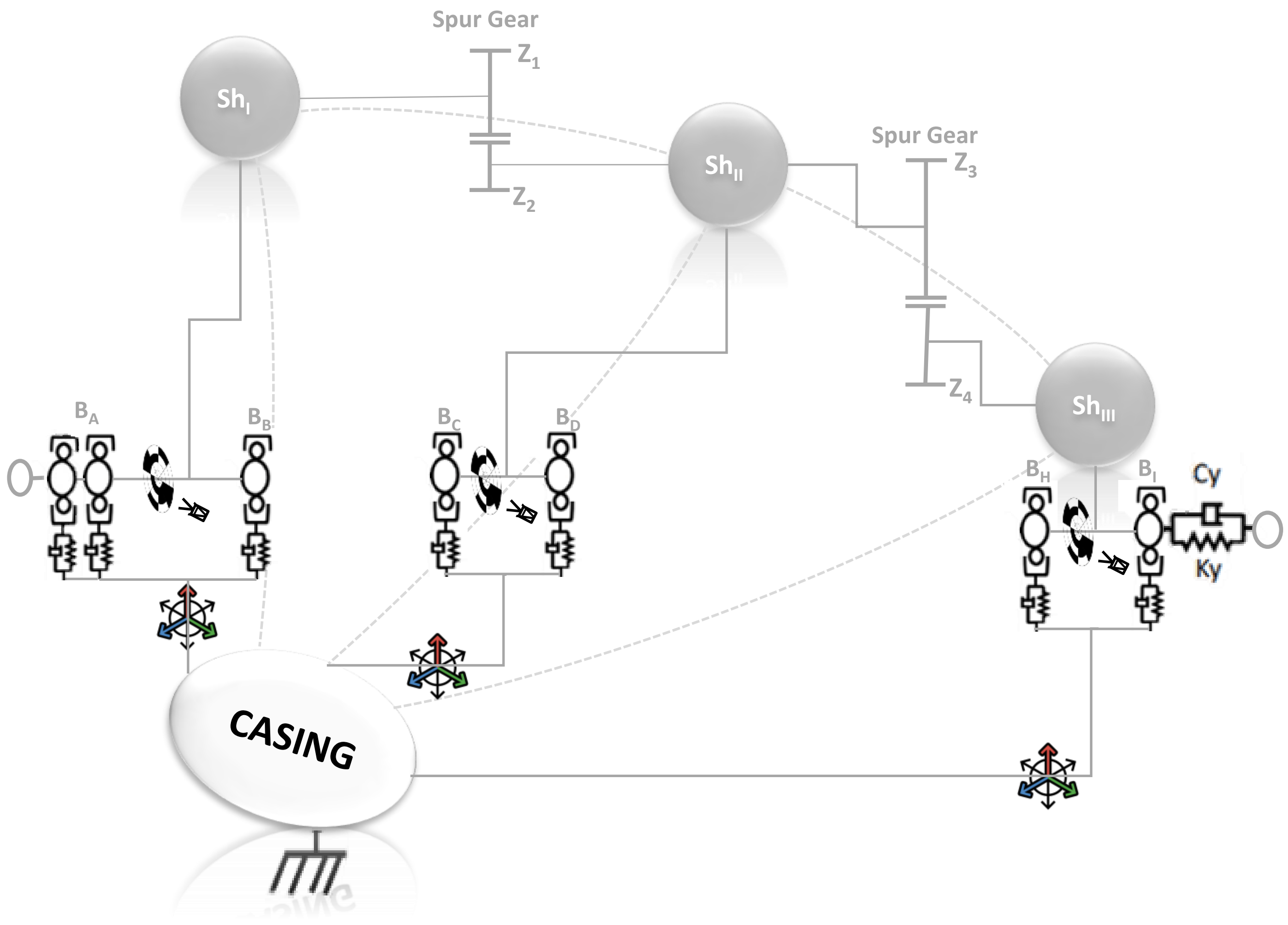


Accelerometer


Optical Encoder

Graph Theory:2-Stage Gear Box

Layer 4 – Virtual Sensor

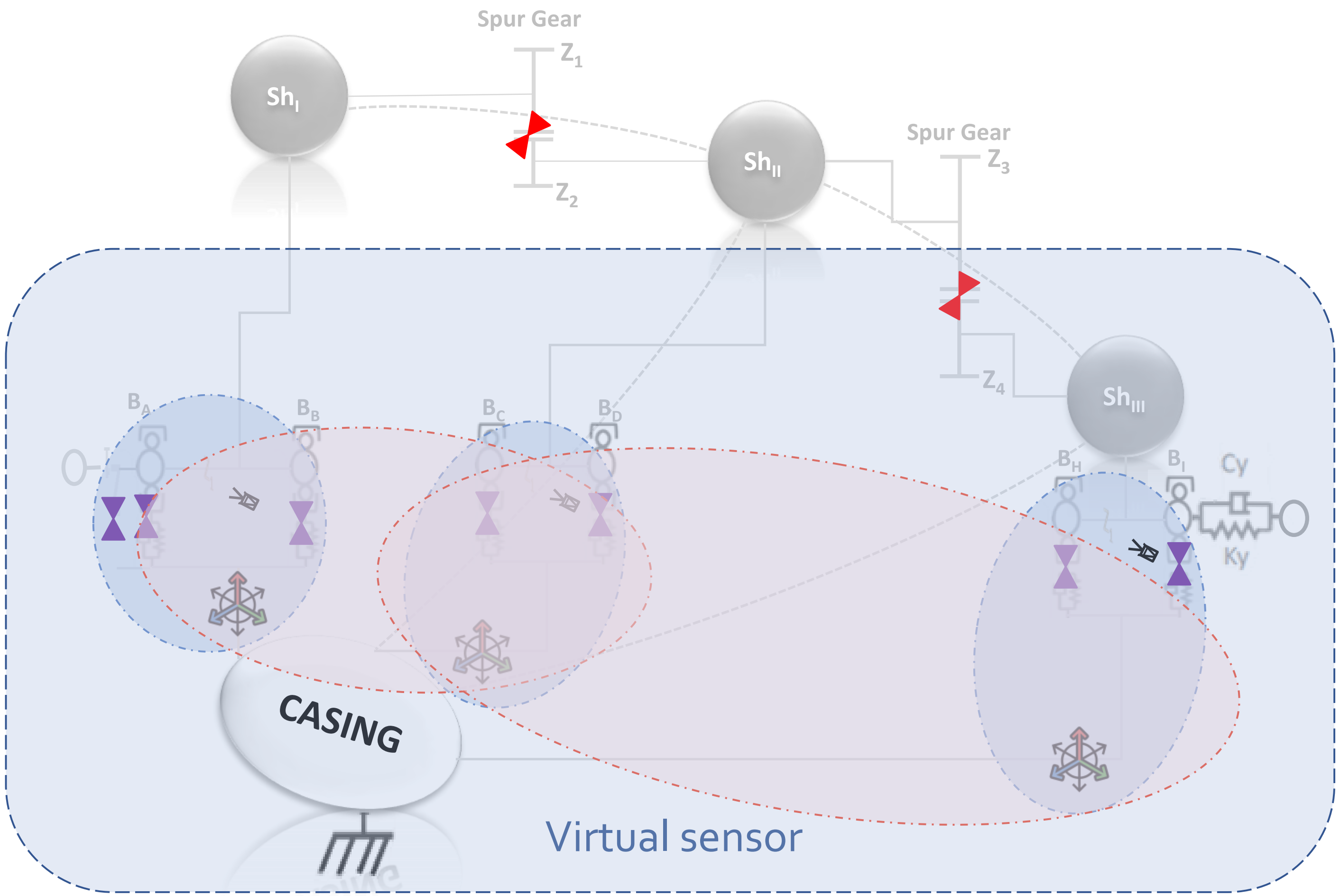

Effective Identification of Cyclic and Resonance Excitations:

$$
\begin{cases}
M_1 \cdot \ddot{x}_1 + C_1 \cdot \dot{x}_1 + K_1 \cdot x_1 = -F_g \cdot (1 + \beta \cdot sin(z_1 \cdot \theta_1)) \\
M_2 \cdot \ddot{x}_2 + C_2 \cdot \dot{x}_2 + K_2 \cdot x_2 = F_g \cdot (1 + \beta \cdot sin(z_1 \cdot \theta_1)) \\
I_1 \cdot \ddot{\theta}_1 + C_{r_1} \cdot \dot{\theta}_1 = \|T_M\| - R_{b1} \cdot F_g \cdot (1 + \beta \cdot sin(z_1 \cdot \theta_1)) + T_{ex1} \\
I_2 \cdot \ddot{\theta}_2 + C_{r_2} \cdot \dot{\theta}_2 = \|T_R\| - R_{b2} \cdot F_g \cdot (1 + \beta \cdot sin(z_1 \cdot \theta_1))
\end{cases}
$$

$$F_{Gear} = F_g \cdot (1 + \underbrace{\beta \cdot sin(z_1 \cdot \theta_1)}_{\text{Fluctuation}}) \quad \& \quad T_{ex1} = C_R \cdot t + C_S \cdot \sin(\omega(t) \cdot t)$$

$$F_g = K_g \cdot (R_{b1} \cdot \theta_1 + R_{b2} \cdot \theta_2) + C_g \cdot (R_{b1} \cdot \dot{\theta}_1 + R_{b2} \cdot \dot{\theta}_2) + K_g \cdot (x_1 - x_2) + C_g \cdot (\dot{x}_1 - \dot{x}_2)$$

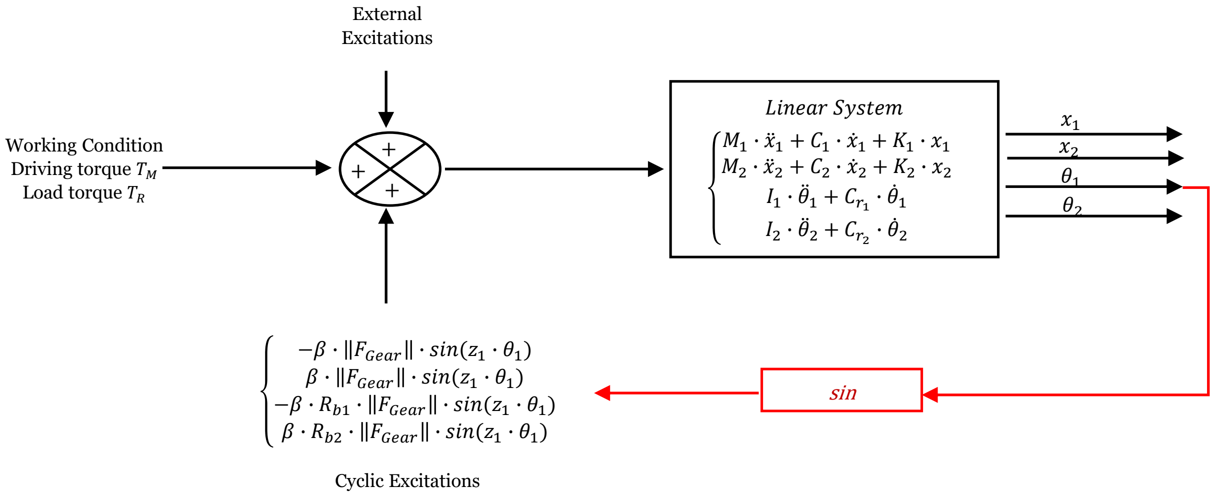

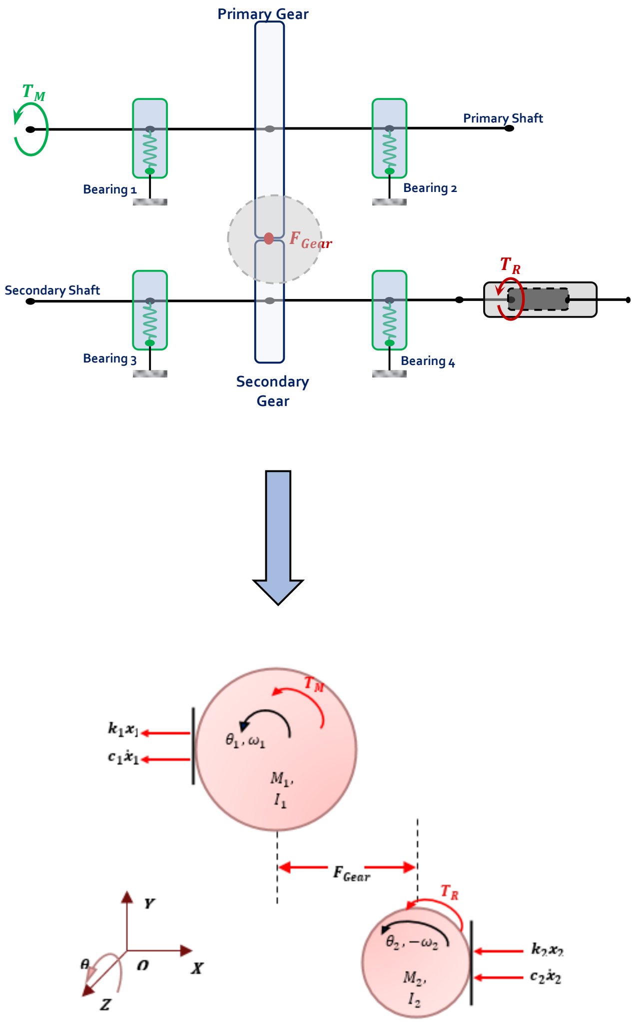

➢ Modal Parameters Identification in Frequency Domain

Algorithm using **complex Frequency Response Function (FRF)** of a **MIMO** system

Based on :

- the Least Square Complex Frequency Estimator (LSCF)

→ stabilization chart in a specified order range →
- eigenfrequency,
- modal damping factor
- identified FRF (discrete z-model)

- The Least-Squares Frequency-Domain estimator (LSFD)

→
- complex residues
- identified FRF using s-model

Advantages :

- produces "fast stabilizing" stabilization charts:
- use of **frequency-dependent weighting functions** (the inclusion of weights in the Least Squares cost function allows to improve accuracy of the estimates)
- the LSCF estimator can easily be adapted to more sophisticated solvers such as the Generalized Total Least-Squares implementation

Spectrums in Hz, Order, and Angular (Constant average speed):

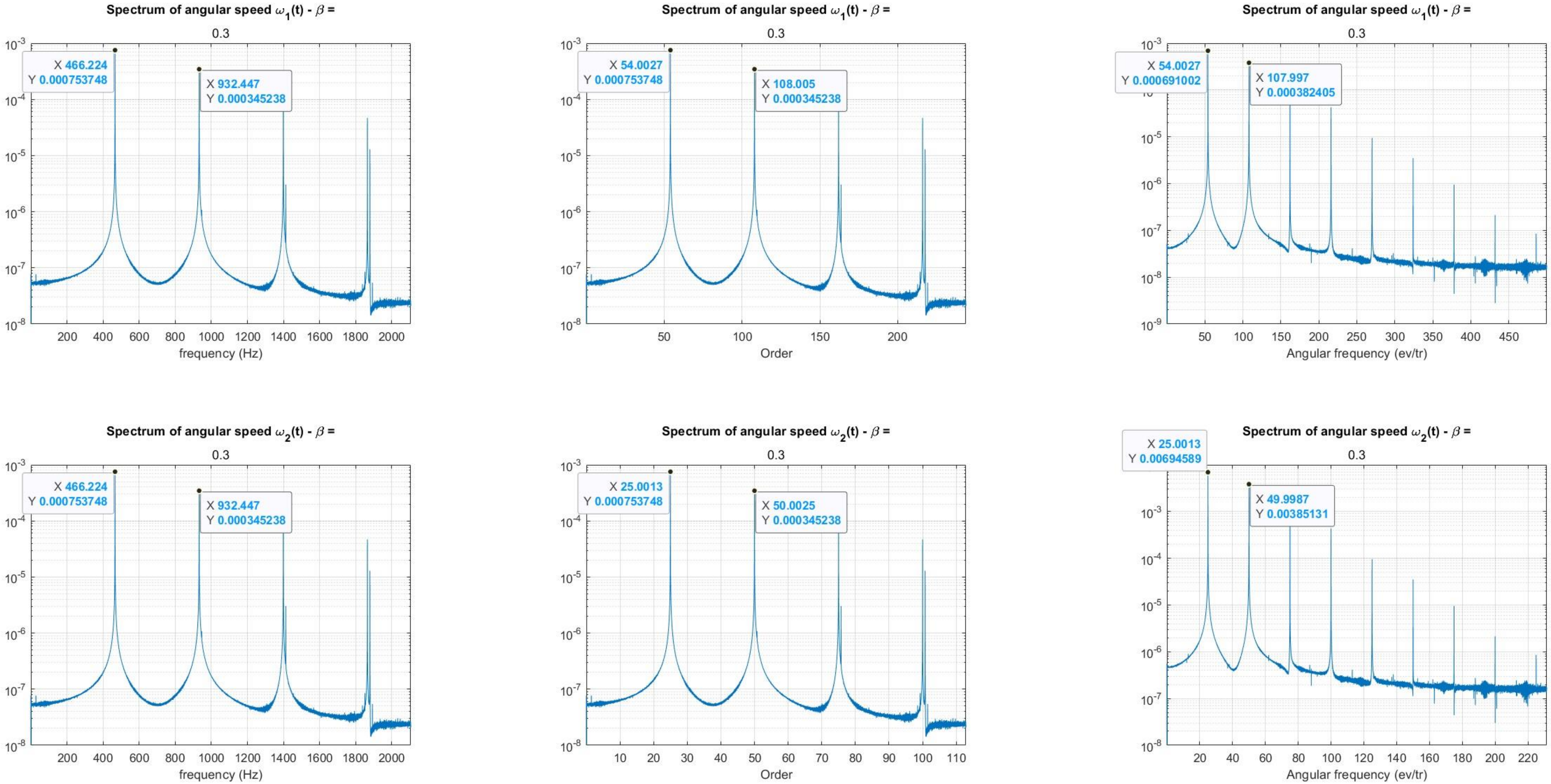

Swept frequency Excitation:

Notations:

- $f_i(t)$ — the user-specified frequency sweep
- $f_{i(actual)}(t)$ — the actual output frequency sweep, usually equal to $f_i(t)$
- $y(t)$ — the Chirp block output

$$y(t) = \cos(\psi(t) + \phi_0)$$

- $\psi(t)$ — the phase of the chirp signal, where $\psi(0) = 0$, and $2\pi f_i(t)$ is the derivative of the phase

$$f_i(t) = \frac{1}{2\pi} \cdot \frac{d\psi(t)}{dt}$$

→ Only holds for:
- **Linear**
- **Quadratic**
- **Logarithmic**

- ϕ_0 — the **Initial phase** parameter value, where $y_{chirp}(0) = \cos(\phi_0)$

Equations for Unidirectional Positive Sweeps:

$$f_i(t) = \frac{1}{2\pi} \cdot \frac{d\psi(t)}{dt}$$

Frequency Sweep	Block Output Chirp Signal	User-Specified Frequency Sweep, $f_i(t)$	β	Actual Frequency Sweep, $f_{i(actual)}(t)$
Linear	$y(t) = \cos(\psi(t) + \phi_0)$	$f_i(t) = f_0 + \beta \cdot t$	$\beta = \frac{f_i(t_g) - f_0}{t_g}$	$f_{i(actual)}(t) = f_i(t)$
Quadratic	Same as Linear	$f_i(t) = f_0 + \beta t^2$	$\beta = \frac{f_i(t_g) - f_0}{{t_g}^2}$	$f_{i(actual)}(t) = f_i(t)$
Logarithmic	Same as Linear	$f_i(t) = f_0(\frac{f_i(t_g)}{f_0})^{\frac{t}{t_g}}$ $Where\, f_i(t_g) > f_0 > 0$	N/A	$f_{i(actual)}(t) = f_i(t)$
Swept cosine	$y(t) = \cos(2\pi f_i(t)t + \phi_0)$	Same as Linear	Same as Linear	$f_{i(actual)}(t) = f_i(t) + \beta t$

➢ **Logarithmic** Instantaneous Frequency Sweep Rate:

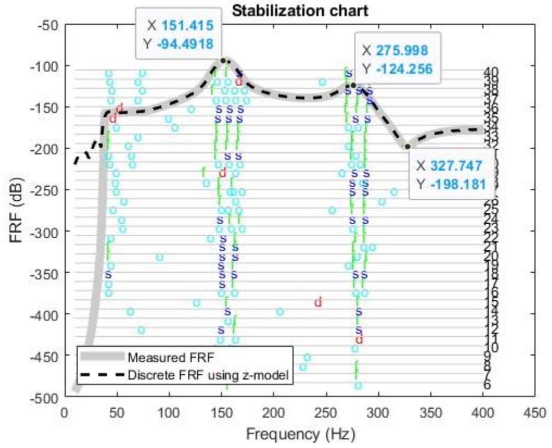

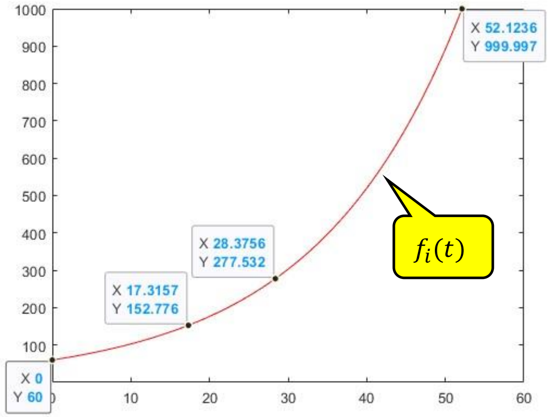

➢ **Linear** Instantaneous Frequency Sweep Rate:

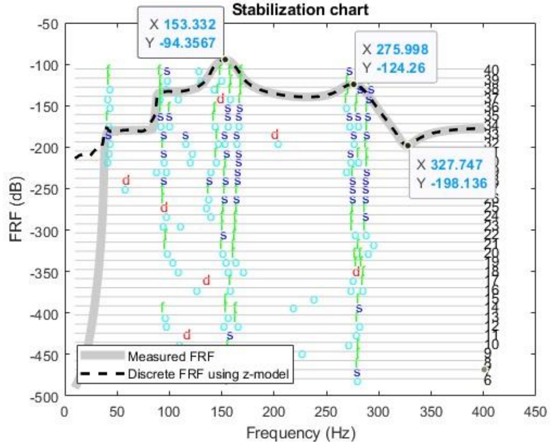

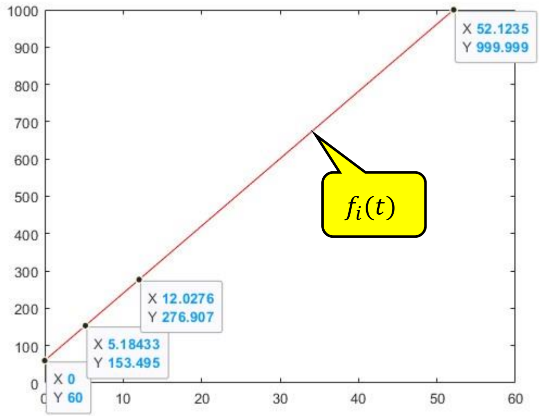

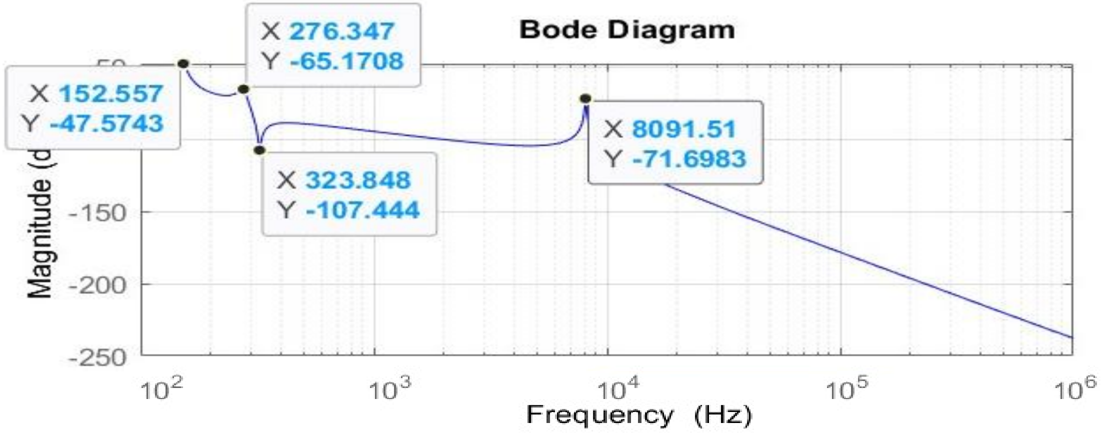

➢ A. Using “**Cyclic external perturbation**” + **Ramp** for excitation :

- Constant Gear Mesh Stiffness ($\boldsymbol{K_g = 1.8 \cdot e^8}$)
- **Without** cyclic fluctuation ($\beta = 0$)

$$\begin{cases} M_1 \cdot \ddot{x}_1 + C_1 \cdot \dot{x}_1 + K_1 \cdot x_1 = -F_g \\ M_2 \cdot \ddot{x}_2 + C_2 \cdot \dot{x}_2 + K_2 \cdot x_2 = F_g \\ I_1 \cdot \ddot{\theta}_1 + C_{r_1} \cdot \dot{\theta}_1 = \|T_M\| - R_{b1} \cdot F_g + T_{ex1} \\ I_2 \cdot \ddot{\theta}_2 + C_{r_2} \cdot \dot{\theta}_2 = \|T_R\| - R_{b2} \cdot F_g \end{cases}$$

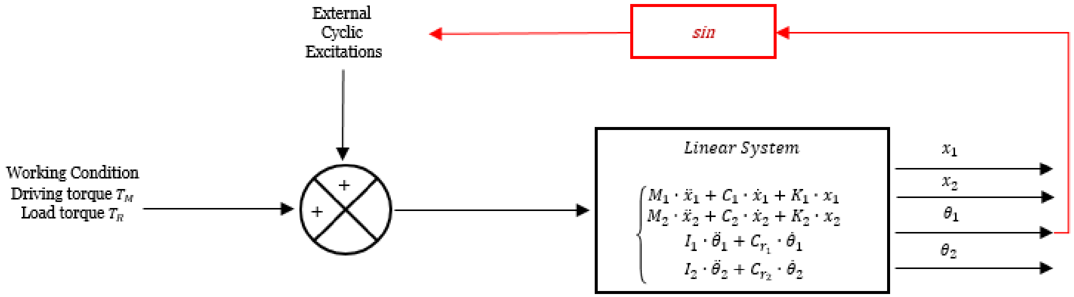

To have cyclic excitation, depending on the angular position of the shaft:

$$T_{ex1} = C_S \cdot sin\left(f_{ev/tr} \cdot \theta_1(t)\right) + C_R \cdot t$$

Once we can use analogy and write ($\phi_0 = 0$):

$$y(t) = \cos\left(f_{ev/tr} \cdot \theta_1(t)\right)$$

Then the Instantaneous Frequency $f_i(t)$ becomes:

$$f_i(t) = \frac{f_{ev/tr}}{2\pi} \cdot \frac{d\theta_1(t)}{dt} = \frac{f_{ev/tr}}{2\pi} \cdot \dot{\theta}_1(t)$$

Case A.1:

- $T_{ex1} = C_S \cdot sin\left(f_{ev/_{tr}} \cdot \theta_1(t)\right) + C_R \cdot t$
- $C_S = 50 \;\; \& \;\; C_R = 10 \;\;\; \& \;\;\; f_{ev/_{tr}} = 1$

According to the plot of the Frequency pf the Rotation:

$$\begin{cases} \bullet \; f_0 = 9.31 \; hz \\ \bullet \; t_g = 52.1235 \; s \\ \bullet \; f_i(t_g) = 32.58 \; hz \end{cases}$$

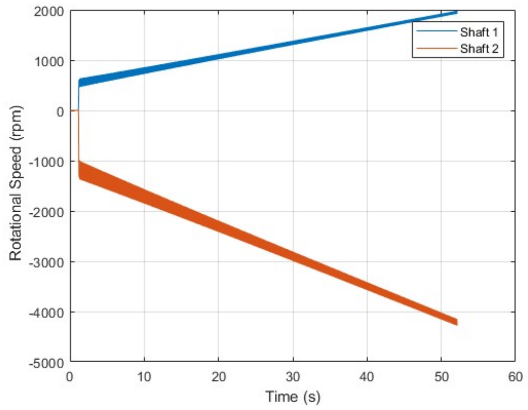

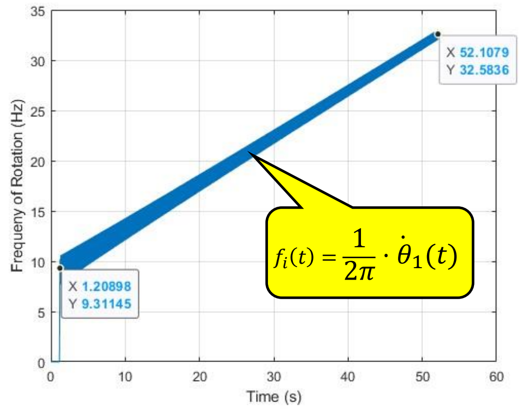

- Since the frequency bandwidth covered by the Instantaneous frequency is not relevant to bandwidth of interest, the FRF estimation is not good!
- To cover a correct frequency bandwidth, the slope of ramp (C_R) needs to increase.

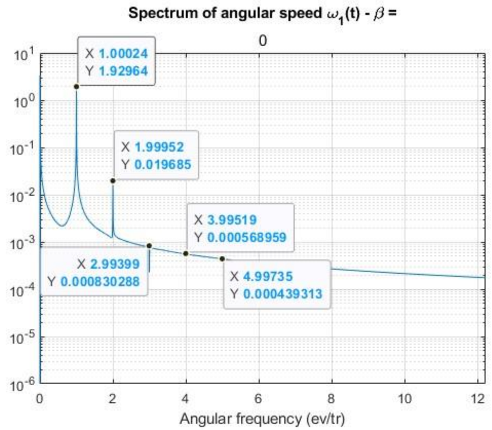

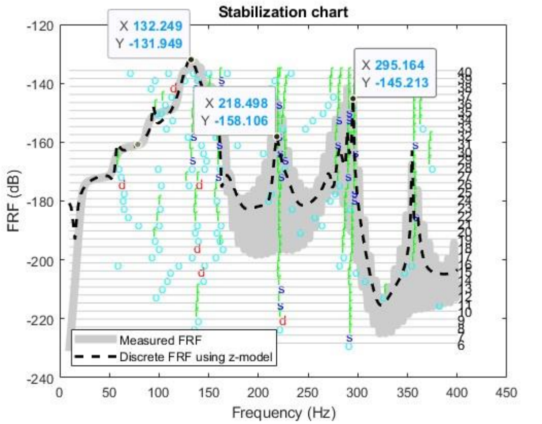

Case A.2:

- $T_{ex1} = C_S \cdot sin\left(f_{ev/_{tr}} \cdot \theta_1(t)\right) + C_R \cdot t$
- $C_S = 50$ & $C_R = 100$ & $f_{ev/_{tr}}=1$

According to the plot of the Frequency pf the Rotation:

- $f_0 = 14.006\ hz$
- $t_g = 52.1235\ s$
- $f_i(t_g) = 247.642\ hz$

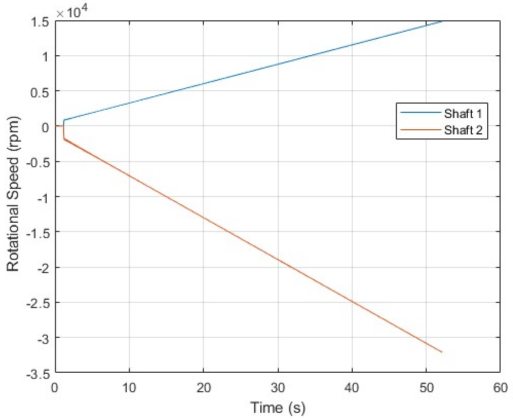

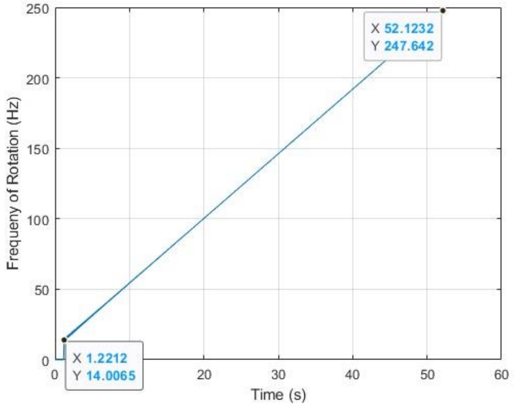

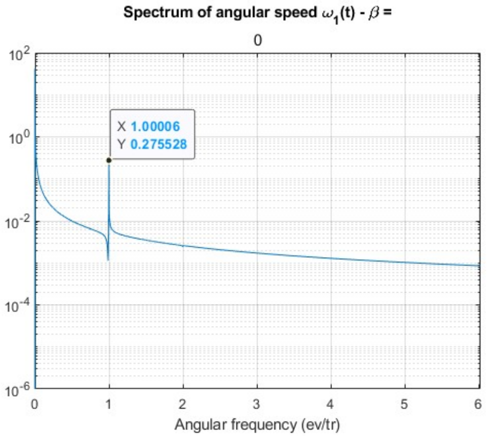

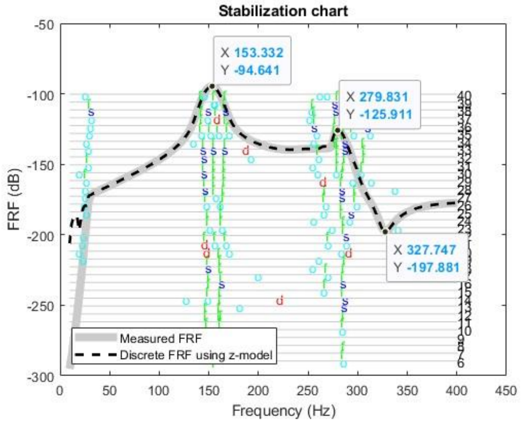

- Although the maximum frequency covered by the Instantaneous frequency is lower than the second resonance, but due to the transient response the FRF estimation is good enough!

B. Non-linear gear interaction:

$$\begin{cases} M_1 \cdot \ddot{x}_1 + C_1 \cdot \dot{x}_1 + K_1 \cdot x_1 = -F_g \cdot (1 + \beta \cdot sin(z_1 \cdot \theta_1)) \\ M_2 \cdot \ddot{x}_2 + C_2 \cdot \dot{x}_2 + K_2 \cdot x_2 = F_g \cdot (1 + \beta \cdot sin(z_1 \cdot \theta_1)) \\ I_1 \cdot \ddot{\theta}_1 + C_{r_1} \cdot \dot{\theta}_1 = \|T_M\| - R_{b1} \cdot F_g \cdot (1 + \beta \cdot sin(z_1 \cdot \theta_1)) + T_{ex1} \\ I_2 \cdot \ddot{\theta}_2 + C_{r_2} \cdot \dot{\theta}_2 = \|T_R\| - R_{b2} \cdot F_g \cdot (1 + \beta \cdot sin(z_1 \cdot \theta_1)) \end{cases}$$

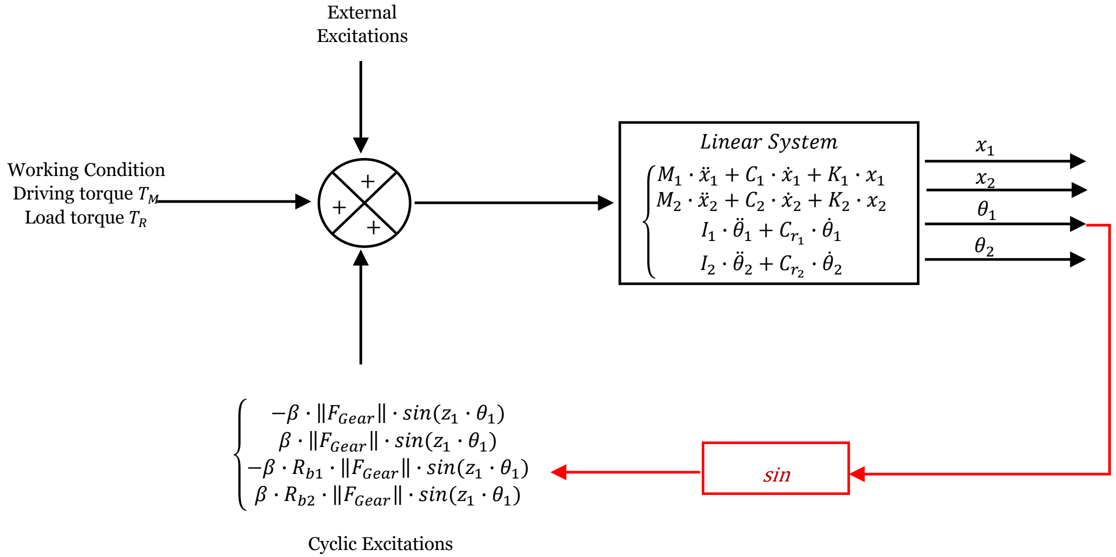

- Varying Gear Mesh Stiffness (K_g)
- **With** cyclic fluctuation ($\beta = 0.3$)
- The external excitation (T_{ex1}) was chosen as: $T_{ex1} = C_R \cdot t$

i.
- $T_M = 1 \cdot 266\ N \cdot m$
- $C_R = 30$
- $450\ rev$

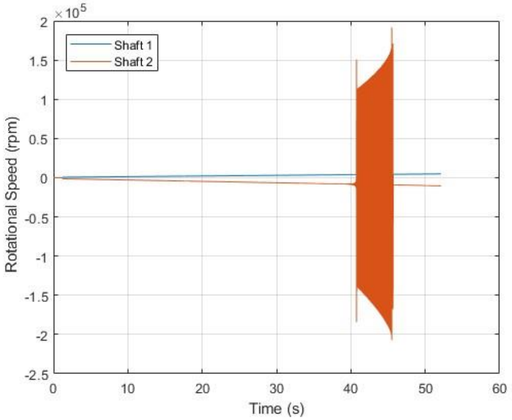

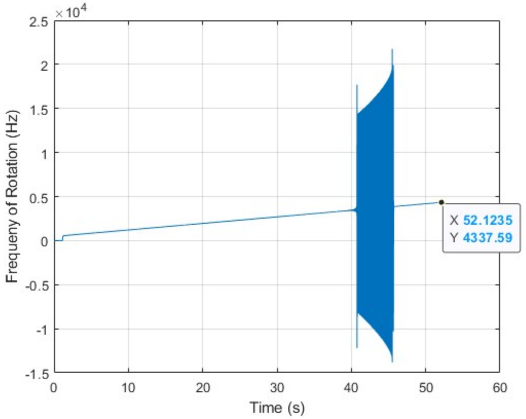

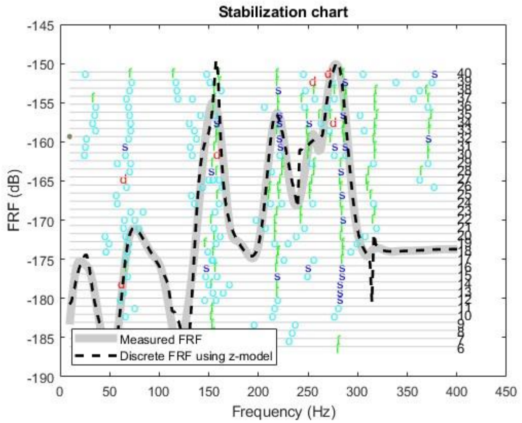

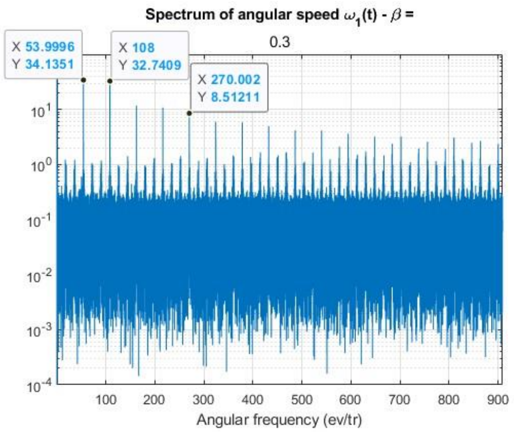

ii.
- $T_M = 1 \cdot 266\ N \cdot m$
- $\boldsymbol{C_R = 100}$
- $450\ rev$

iii.
- $T_M = 1 \cdot 266\ N \cdot m$
- $C_R = 100$
- $\boldsymbol{300\ rev}$

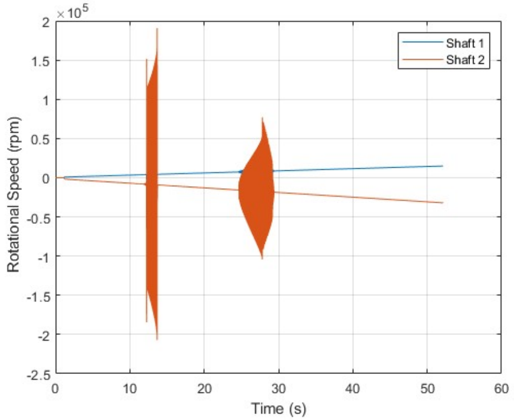

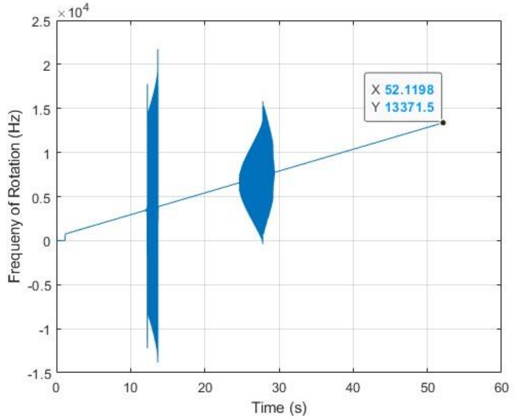

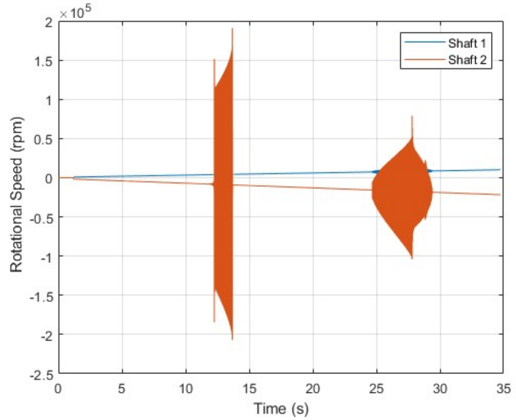

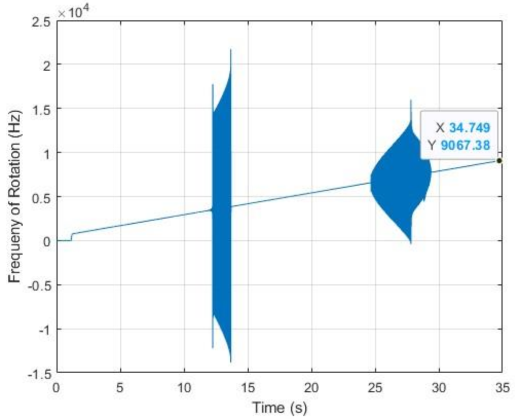

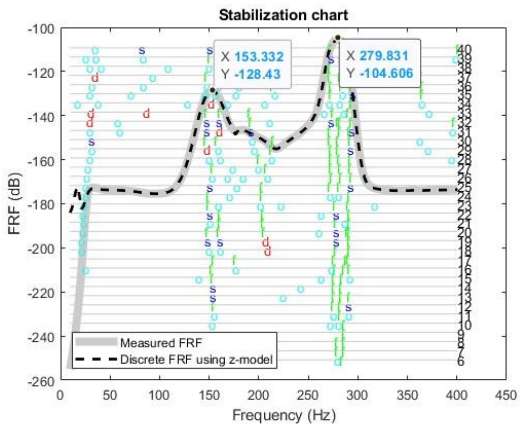

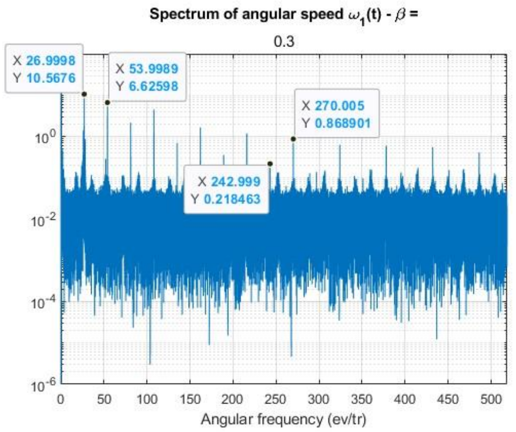

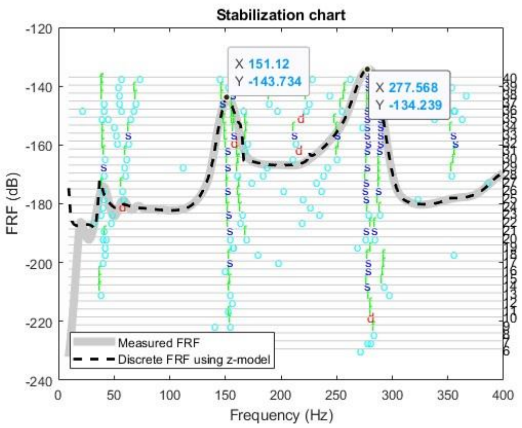

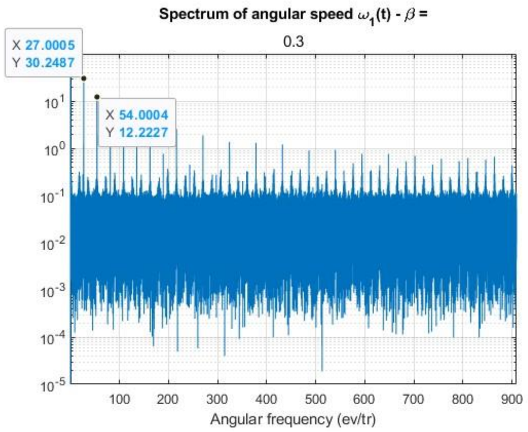

$iv.$
- $\boldsymbol{T_M = 0.25 \cdot 266\ N \cdot m}$
- $\boldsymbol{C_R = 30}$
- $\boldsymbol{900\ rev}$

$v.$
- $T_M = 0.25 \cdot 266\ N \cdot m$
- $C_R = 30$
- $\boldsymbol{600\ rev}$

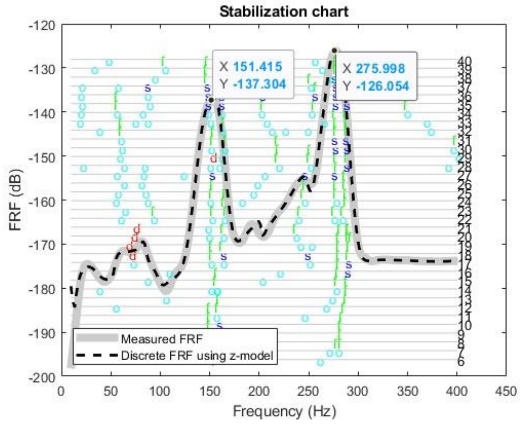

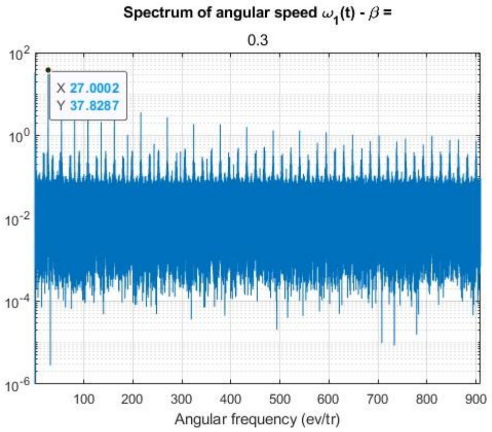

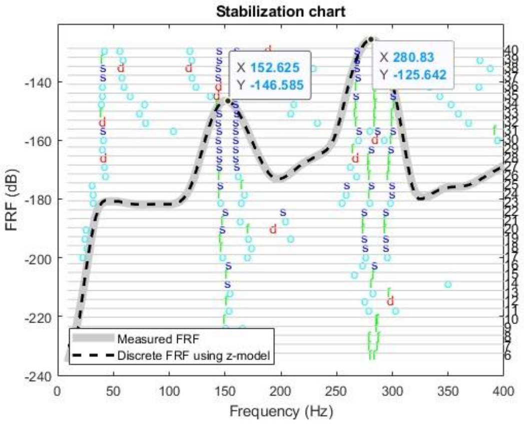

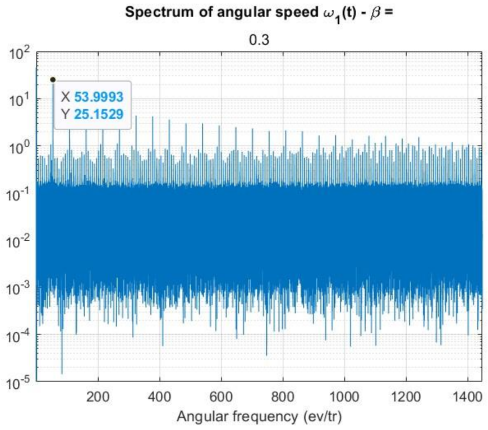

C. Both the Non-linear gear interaction with external cyclic perturbation:

- Varying Gear Mesh Stiffness (K_g)
- **With** cyclic fluctuation ($\beta = 0.3$)
- External excitations are a cyclic perturbation, and a ramp in torque!

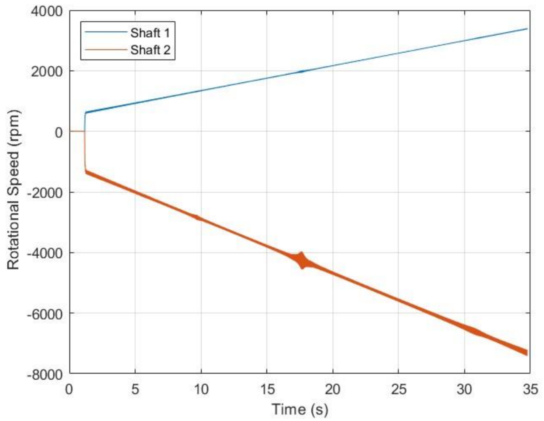

Case C.1:

$$T_{ex1} = C_S \cdot sin\left(f^{ev}/_{tr} \cdot \theta_1(t)\right) + C_R \cdot t, \qquad C_S = 50 \;\; \& \;\; C_R = 30$$

The Driving Torque: $T_M = 1 \cdot 266\ N \cdot m$

cyclic frequency $f^{ev}/_{rev} = 3$

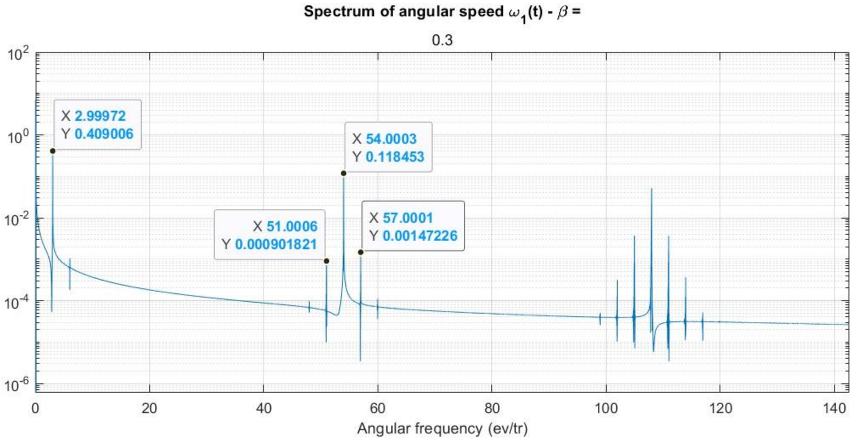

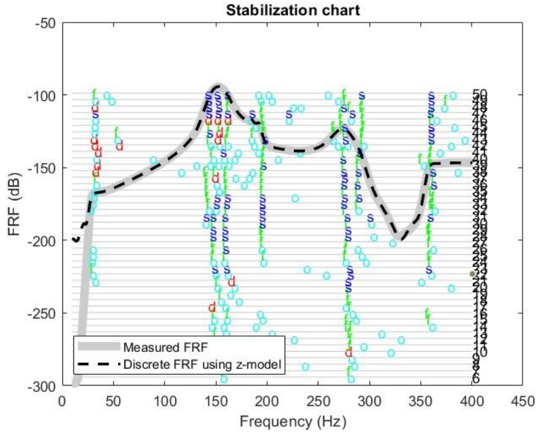

➢ C. Both the Non-linear gear interaction with external cyclic perturbation:

- Case C.2:

$$T_{ex1} = C_S \cdot sin\left(f^{ev}/_{tr} \cdot \theta_1(t)\right) + C_R \cdot t, \qquad C_S = 50 \;\; \& \;\; C_R = 30$$

The Driving Torque: $T_M = 0.25 \cdot 266\ N \cdot m$

cyclic frequency $f^{ev}/_{rev} = 3$

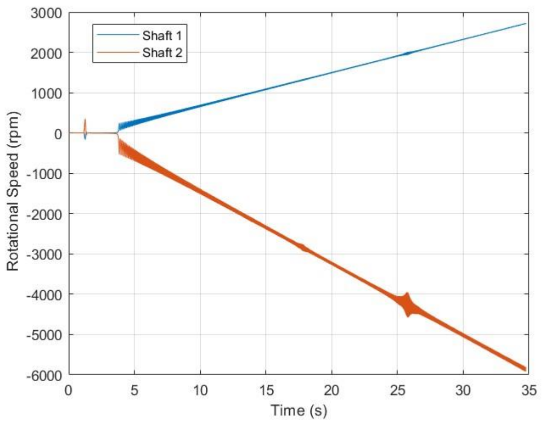

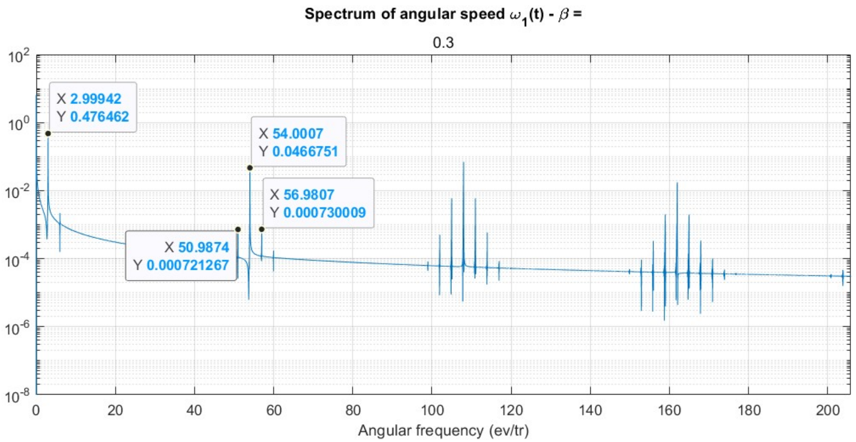

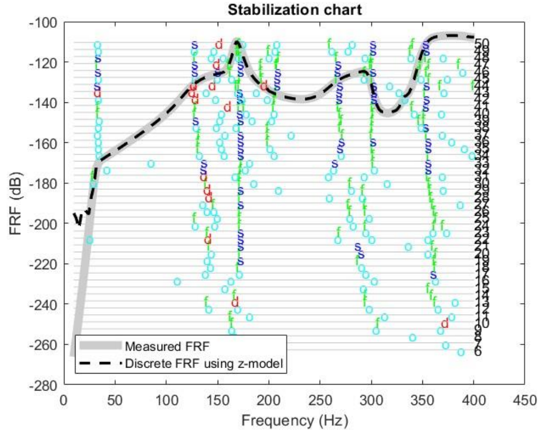

Questions:

In the presence of large frequency values, why half the fundamental harmonic appears? might be due to:

- Sampling: Not only coarse sampling induces error (Aliasing error), but also very fine sampling might cause difficulties too – what is the criterion for the upper limit of frequency sampling?
- Non-linear interaction inside the system? How to avoid it?

Thank You
For Your Attention

Introduction to the identification approaches

Time – Domain

Orthogonal Functions

- Expanding of excitation and response signals in the polynomial basis
- Using integration and derivation property of the orthogonal functions
- so-called operational matrix of respectfully integration and derivation

→ **Differential equations can be transformed into algebraic equations**

Basis:

- **Chebyshev Polynomials**
- **Fourier Series**
- **Block-Pulse Functions**
- **Shifted Legendre Functions**

Book:

"**Modelling and Identification with Rational Orthogonal Basis Functions**" Springer, London. 2005